Saudi Pharmaceutical Journal 31 (2023) 101689

HOSTED BY

Contents lists available at ScienceDirect

Saudi Pharmaceutical Journal

journal homepage: www.sciencedirect.com

Original article

Solid lipid Lyo-Nanosuspension: A promising stabilized oral delivery system for the antihyperglycemic extract of mistletoe *Plicosepalus acacia*

Samar Zuhair Alshawwa [a], Gihan Salah Labib [b], Shaimaa M. Badr-Eldin [c,d], Abeer Ahmed Kassem [b,*]

[a] Department of Pharmaceutical Sciences, College of Pharmacy, Princess Nourah bint Abdulrahman University, P.O.Box 84428, Riyadh 11671, Saudi Arabia
[b] Department of Pharmaceutics and Pharmaceutical Technology, Faculty of Pharmacy, Pharos University in Alexandria, 21321 Alexandria, Egypt
[c] Department of Pharmaceutics, Faculty of Pharmacy, King Abdulaziz University, Jeddah 21589, Saudi Arabia
[d] Department of Pharmaceutics and Industrial Pharmacy, Faculty of Pharmacy, Cairo University, Cairo, 11562, Egypt

ARTICLE INFO

Article history:
Received 15 April 2023
Accepted 20 June 2023
Available online 26 June 2023

Keywords:
Dry Solid Lipid
Nanosuspension
Antihyperglycemic
Lyophilized
Plicosepalus acaciae extract

ABSTRACT

The antihyperglycemic effect of *Plicosepalus acaciae* (*P. acaciae*) extract was proven, but it still needs to be formulated into a suitable dosage form. We aimed at preparing an oral stabilized SLNs for *P. acaciae* with high payload, to be used as powder for reconstitution, filled into capsule or compressed into tablet. SLNs were prepared by emulsion solvent evaporation technique. Preliminary characterization was performed followed by full assessment of the optimized SLNs suspension and/or its lyophilized form: particle size, zeta potential, surface morphology, percentage entrapment efficiency (% EE), DSC, FTIR and in vitro release studies. The optimized SLNs lyophilized formula ($F3_L$) exhibited acceptable compressibility and flowability. The reconstituted F3L showed % sedimentation volume of 91.83 %, re-dispersibility of 95%, viscosity of 764.33 cp, uniform particle size of 30.28 nm as shown by TEM, polydispersity index (PDI) of 0.16, zeta potential of −36.4 mV, % EE of 89.64 % and drug content of 97.69 %. The physical mixture and $F3_L$ FTIR spectrum indicated compatibility of components. In vitro release study showed a burst release in lyophilized formulations followed by slow-release, calculated as total phenolic content. Our previously reported work revealed that the total extracts of *P. acaciae* and SLNs formulations with the greatest lipid content $F3_s$, demonstrated a considerable blood glucose-lowering effect in diabetic rats. The obtained lyophilized SLNs is promising for preparation of a suitable stable dosage form for *P. acaciae* extract to be used in treatment of diabetes.

1. Introduction

Diabetes mellitus is a chronic metabolic disorder attributable to insulin resistance or progressive pancreatic beta cell failure and lack of insulin secretion. Oral drug delivery, being a non-invasive easy way for drug administration is still considered the most preferred common route that increases patient compliance with high therapeutic efficacy. Reduction in blood glucose levels is achieved through oral anti-diabetic drugs by either enhancing insulin sensitivity or initiating insulin secretions (Mukherjee et al., 2020; Shazhni et al., 2018). However, the hydrophilic environmental condition of the gastrointestinal tract, renders the bioavailability of some poorly water-soluble drugs limited (Chakraborty et al., 2009). Drug delivery systems comprising lipids have been recognized in the few past decades for being an effective tool as absorption enhancer (Porter et al., 2007). Among lipid based colloidal drug delivery systems are the solid lipid nanoparticles (SLNs). They were first introduced in 1991 as an alternative drug carrier to traditional colloidal systems as emulsions, nano-emulsions, polymeric micro and nano-particles and liposomal carriers (R. H. Müller et al., 2000). SLNs are characterized by being solid at both body and room temperature (Silva et al., 2011). In comparison to other known colloidal drug delivery systems, they are more preferred owing to their reported advantages comprising; lower cytotoxicity, higher drug stability, increased bioavailability, biodegradability, and appropriate tolerability (Mehnert & Mäder, 2012; Mukherjee et al., 2007; R. Müller et al., 1996). Multiparticu-

* Corresponding author.
E-mail addresses: szalshawwa@pnu.edu.sa (S. Zuhair Alshawwa), gihan.labib@-pua.edu.eg (G. Salah Labib), smbali@kau.edu.sa (S.M. Badr-Eldin), abeer.kassem@-pua.edu.eg, abeerkassem2002@gmail.com (A. Ahmed Kassem).

Peer review under responsibility of King Saud University. Production and hosting by Elsevier.

Production and hosting by Elsevier

https://doi.org/10.1016/j.jsps.2023.06.022
1319-0164/

late systems, e.g., powder, or granules could be prepared from solid lipid formulations and filled into capsules or sachets, or either compressed into tablets using suitable excipients to improve their flowability and avoid sticking to the punches and die cavity (Chakraborty et al., 2009). SLNs are generally prepared using solid lipids and stabilized using surfactants. *Plicosepalus acaciae* (*P. acaciae*), previously known as Loranthus, is a mistletoe (hemi-parasitic plant belong to several families) (Leitão et al., 2013). It is an abundant plant all over Saudi Arabia and was traditionally used for decades in several variant neurological and cardiovascular related disease conditions (Kelsey et al., 2010; Kim et al., 2004; Sasidharan et al., 2010; Shargorodsky et al., 2010). Recent studies approved its cytotoxic (Lalitha et al., 2020), gastroprotective (M. A. Abbas et al., 2019), antimicrobial (Moglad, 2021) and wound healing activities (Moglad et al., 2020). The antidiabetic activity of *P. acaciae* was also investigated and documented (Aldawsari et al., 2014; El-Sayed et al., 2020; O. M. Noman et al., 2019; Osadebe et al., 2004; Sadi & Güray, 2009). *P. acaciae* showed a prophylactic action and a successful treatment for diabetes mellitus because of its anti-inflammatory, antioxidant, hypoglycemic, hypolipidemic and insulin secretagogue effects. Its regenerative and protecting impact on pancreatic β cells was assigned to activating β- cells signaling, which lead to enhanced glucose and lipid metabolism (El-Sayed et al., 2020).

The aim of the current work was to assess the suitability of the prepared SLNs suspension and lyophilized powder for the encapsulation of *P. acaciae* extract, in addition to characterization and evaluation of the prepared formulations. The second aim was to show how our formula of choice was selected for its in vivo antidiabetic effect on diabetic rats that was previously proved and published (Aldawsari et al., 2014). We recommend suspension for reconstitution as a dosage form for *P. acaciae* extract and/or tablet or capsule as a more stable forms for the lyophilized powder. So that sedimentation volume, re-dispersibility and viscosity of the ready prepared and reconstituted SLNs suspension formulations were studied. In addition, compressibility and flowability parameters for the lyophilized powder were assessed.

2. Materials and methods

2.1. Materials

Compritol® 888 ATO was given by Gattefosse Corporation (Paramus, NJ, USA). Pearlitol® (spray-dried mannitol) was kindly donated by Roquette (Nord-Pas-de-Calais, France). Sodium dodecyl sulfate (SDS) was bought from Sigma Aldrich (St. Louis, MO, USA). Chloroform was obtained from Fisher Scientific Co. (Norcross, GA, USA). Other chemicals were of analytical grade.

2.2. Plant collection and preparation of extract

Whole plants of *P. acaciae* (Zucc.) Wiens & Polhill was collected from the northwestern area of Saudi Arabia in March, identified in Faculty of Science, King Abdulaziz University (KAU), Jeddah, KSA, registered under the code of "2010-PA1", dried and extracted by the specialized laboratory techniques at the natural products department, College of Pharmacy, KAU, as being previously reported and published by the author in details (Aldawsari et al., 2014).

2.3. Determination of total phenolic compound

The total phenolic content for *P. acaciae* was determined spectrophotometrically at 764 nm (Ultraviolet-Spectrophotometer, Pharmacia Biotech, double beam, Cambridge, England) using the Folin–Ciocalteu method (FC), as has previously been reported and discussed in details for the determination of total phenolic compounds in pharmaceutical dosage forms (El Hajaji et al., 2010; Labib & Aldawsari, 2015). 25 mg of the extract was dissolved 10 mL methanol. Twenty microliters' aliquots were sampled using a calibrated micropipette and added to 100 uL of FC reagent. After eight minutes of the reaction, 300 µL 25% saturated sodium carbonate aliquot was added to the samples. The absorbance was then measured after suitable dilutions at 764 nm against a calibration curve using Gallic acid as equivalent standard in the range from 0 to 500 mg/L concentrations. Triplicates were done and an average total phenolic content was determined ± SD.

2.4. Preparation of nanosuspension loaded with mistletoes *Plicosepalus acaciae*

Solid lipid nanoparticles were prepared by emulsion-solvent evaporation technique as has been previously reported (Aldawsari et al., 2014; Rahman et al., 2006). 500 mg of *P. acaciae* and different predetermined amounts of Compritol® 888 ATO were dissolved in 10 mL of chloroform and dropped into 20 mL of 0.05 % aqueous solution of SDS at a rate of 10 drops /min under homogenization speed of 6000 rpm using probe type homogenizer (PowerGen 125, Fisher Scientific, PA, USA) for 10 min (Table 1). The created colloidal lipid *sol* was then mechanically stirred at 1000 rpm for 2 h with the objective of evaporating the organic solvent, so that the final volume of all preparations was 20 mL. Formulations were prepared in duplicates for each, where one was kept as a readily constituted suspension ($F1_s$, $F2_s$ and $F3_s$) and the other was subjected to freeze drying to be reconstituted on use ($F1_L$, $F2_L$ and $F3_L$). The latter formulations were frozen at −80C after adding 1% Pearlitol® as cryo-protectant, then they were subjected to lyophilization till a completely dried powder was produced (24 h). The powdered formulations were kept in airtight amber glass wide mouth bottles pending further characterization.

2.5. Preliminary characterization of SLNs suspension

2.5.1. Sedimentation volume

Sedimentation volume was determined according to a previously reported method (Rani & Hema, 2014). 25 mL measuring cylinder was filled with 20 mL of the prepared suspension or redispersed lyophilized suspension after reconstitution. The suspension was allowed to be dispersed by shaking the cylinder upside down three times and initial sediment volume (V_0) was measured. The suspension was permitted to stand for 24 h whereupon the volume of sediment (V_u), was measured.

% Sedimentation volume (F) was calculated from the relation:

$$F = \frac{Vu}{V0} * 100$$

Experiments were conducted in triplicate.

2.5.2. Re-dispersibility assessment

20 mL of the SLNs suspensions or redispersed lyophilized suspension after reconstitution were allowed to free settle in a measuring a 25 mL cylinder for 24 h. Cylinders' mouths were closed, inverted 180° and the number of inversions necessary for 100% re-dispersion was determined for each formulation. (Rani & Hema, 2014). If consistency achieved in one inversion, then it has 100% re-dispersibility. Any extra inversion reduces the percentage of simplicity of re-dispersibility by 5%. Experiments were conducted in triplicate.

Table 1
Preliminary characterization of both SLNs suspensions and lyophilized SLNs powder.

Formula Code	Composition				% Sedimentation volume ±SD	% Re-dispersibility	Viscosity (cp) ± SD	Compressibility and Flowability of lyophilized SLNs		
	P. acaciae extract (mg)	Compritol® 888 ATO (mg)	SDS 0.05% aqueous solution (mL)	Chloroform (mL)				Angle of repose θ (°)	Hausner's ratio	Carr's index
$F1_s$	500	200	20	10	83.833 ± 0.289	100	158.33 ± 5.312	–	–	–
$F2_s$	500	350	20	10	83.833 ± 0.289	100	306.33 ± 6.018	–	–	–
$F3_s$	500	500	20	10	87.833 ± 0.289	95	605.33 ± 8.73	–	–	–
$F1_L$	500	200	20	10	86.167 ± 0.289	100	168 ± 2.94	23.293	1.218	17.93
$F2_L$	500	350	20	10	87.167 ± 0.289	100	311.333 ± 8.179	23.856	1.2	16.67
$F3_L$	500	500	20	10	91.833 ± 0.289	95	764.333 ± 7.587	23.656	1.171	14.615

$_S$ represents the SLNs suspension form, $_L$ represents the lyophilized SLNs powder.

2.5.3. Viscosity measurement

The viscosity of 20 mL ready prepared and reconstituted SLNs suspension preparations was determined at 25 °C utilizing Brookfield viscometer (DV-II + Pro, Brookfield, Middleboro, MA, USA) with spindle number S-03. Measurements were carried at a speed of 100 rpm. Results were taken as an average of three measurements ± SD.

2.6. Preliminary characterization of the lyophilized SLNs powder

As we recommend tablet or capsule for *P. acaciae* extract as a dosage form for the lyophilized powder, compressibility and flowability parameters were evaluated (Hadi et al., 2016; Singh, Salwa, Shirodkar, Verma, & Kumar, 2020). Experiments were conducted in triplicate.

2.6.1. Angle of repose (θ)

An accurately weighed amount of lyophilized SLNs powder was permitted to flow freely through a funnel. The funnel tip height (h) was adjusted to 2 cm from a plane surface. When the apex of the flowing powder touches the funnel tip, the radius (r) of the formed powder cone was measured.

Tan angle of repose (tan θ) was calculated as follows:

$$\tan\theta = \frac{h}{r}$$

2.6.2. Hausner's ratio

Hausner ratio (HR) is the ratio of the tapped bulk density (ρ_t) to the loose bulk density (ρ_b) as follows:

$$HR = \frac{\rho t}{\rho b}$$

Where ρt is the aerated density obtained after freely pouring the lyophilized SLNs powder into 10 mL cylinder (calculated by dividing the powder weight by its aerated volume) and ρb is the constant density obtained during tapping until no further volumes changes occurs (calculated by dividing the powder weight by its tapped volume).

2.6.3. Carr's compressibility index

Carr's Index (%) was calculated by using the following equation:

$$\text{Carr's Index}\,(\%) = \frac{\rho t - \rho b}{\rho t} X\,100$$

2.7. Particle size analysis, zeta potential and surface morphology studies

2.7.1. Zeta sizer measurements

One milliliter sample of the diluted SLNs suspension was used for the measurement of polydispersity index (PDI), particle size (PS) and Zeta potential (ZP) utilizing dynamic light scattering method (Zetatrac: Microtrac, Inc., Montgomeryville, PA, USA).

2.7.2. Transmission electron microscopy (TEM)

Both morphology and the particle size of nanosuspension formulations $F1_s$, $F2_s$ and $F3_s$ were observed by TEM (Jeol 100 CX-transmission electron microscope, Japan). Each sample was made by locating a drop of the nanosuspension that was earlier diluted 50-folds with double-distilled water over a 400-mesh copper grid coated with carbon film and followed by staining with 1% Uranyl acid. The sample was dried in the air earlier to TEM examination.

2.7.3. Scanning electron microscope (SEM)

The shape and surface morphology of lyophilized SLNs were examined utilizing SEM, JSM-5510 (Jeol Ltd, Tokyo, Japan) supplemented with a digital camera. The samples were coated with gold and mounted on a sample holder. The electron micrographs were taken at an accelerating voltage of 5 kV.

2.8. Determination of % encapsulation efficiency (%EE) and drug content

The percentage of encapsulation efficiency (%EE) was determined indirectly by measuring the amount of non-encapsulated drug in the aqueous solution, versus the total amount of drug added to the preparation (Silva et al., 2012). *P. acaciae* loaded SLNs suspensions and reconstituted lyophilized SLNs (2 mL) were placed in a centrifugal ultrafiltration unit (Centrisart® I, pore size 300 kDa NMWCO, Sartorius Stedim Biotech GmbH) and centrifuged in a cooling centrifuge (Model Z 32 HK, Hermle Labortechnik, Germany) at 4500 rpm at 7 °C for 30 min. The free drug passed through the filter membrane and was diluted appropriately, then analyzed for phenolic content using FC method as previously mentioned. Whereas the encapsulated drug remained in the ultrafiltration unit (% EE) was calculated by using the following formula:

$$\text{EE}\,(\%) = \frac{\text{Amount of phenolic content in SLNs}}{\text{Total amount of phenolic content}} X\,100$$

25 mg *P. acaciae* extract and a volume of SLNs suspension or reconstituted lyophilized SLNs powder equivalent to 25 mg *P. acaciae* extract was tested for their *P. acaciae* content. The appropriate amount in each case was completely dissolved in 10 mL methanol, diluted with distilled water and quantified for *P. acaciae* content by determination of the total phenolic content spectrophotometrically at 764 nm using the FC method, as mentioned above. The *P. acaciae* content was calculated using the following formula:

$$\textit{P. acaciae}\,\text{content}\,(\%) = \frac{\text{Amount of phenolic content in SLNs}}{\text{Total phenolic content in extract}} X\,100$$

2.9. In-vitro release and kinetics analysis:

In vitro content release study of the extract, SLNs suspension and reconstituted lyophilized SLNs suspension was performed by dialysis bag diffusion technique using USP type II (paddle) apparatus over 24 h in phosphate buffer pH 6.8, as previously reported with some modifications (Silva et al., 2012). 125 mg extract was suspended in 5 mL medium, a volume of SLNs suspension and reconstituted lyophilized SLNs suspension equivalent to 125 mg extract was individually filled into dialysis bag (Molecular weight cutoff = 12,000 to 14,000 Da; Sigma-Aldrich Corporation**,** St Louis, MO, USA), tightly sealed at both ends and tied in the paddle before immersion into a vessel containing 250 mL of the release medium. Paddle revolution speed was kept over the experimental period at 100 rpm at 37 ± 0.5 °C. The medium was covered to avoid vaporization of water. At preset time increments; 0.25, 0.5, 0.75, 1, 2, 3, 4, 6 and 24 h. 1 mL aliquot was withdrawn and substituted by the same volume of fresh warmed release medium. The results were stated as the mean ± standard deviation (SD) of three replicates (n = 3). The samples were analyzed for *P. acaciae* by determination of the total phenolic content spectrophotometrically at 764 nm using the FC method, as mentioned above. The release profiles of *P. acaciae* from different SLNs suspension formulations and reconstituted lyophilized formulations were compared with that of extract.

The % cumulative amount of total phenolic content released was plotted as a function of time (h).

The mechanism of total phenolic content released from SLNs formulations was investigated using DD solver software. Release data were fitted to four different kinetic models; zero order, first order, Higuchi and Peppas-Korsmeyer (Kumar et al., 2013).

2.10. Differential scanning calorimetry (DSC)

Compritol®, $F3_L$, and P Acaciae were subjected to DSC testing. Five mg samples were accurately weighed, sealed in an aluminum pan, and equilibrated at 25 °C, then subjected to a heating run over the temperature range of 25– 400 °C, using a DSC Q200 (TA instruments, US).

2.11. Fourier transform infrared spectroscopic analysis (FTIR)

SLNs powder, physical mixture, and individual components of the formulation; extract and Compritol® were subjected to both FTIR. FTIR spectra were obtained after compression of each sample as KBr pellets using FTIR spectroscope (Cary 630 FTIR spectroscope, Agilent Technologies, USA) in the range of 4000–400 cm^{-1}.

2.12. In- vivo antidiabetic study of the extract compared to SLNs suspension

Full details of the in-vivo study could be revised in our previously published article (Aldawsari et al., 2014). Briefly, type 2 diabetes was induced in adult male Wistar rats by a high-fat diet accompanied by injection of streptozotocin. The diabetic rats were divided into groups and orally administered, in parallel, the antidiabetic drug pioglitazone hydrochloride, extracts of *P. acaciae*, in addition to the three *P. acaciae* SLNs suspension formulations; $F1_s$, $F2_s$ and $F3_s$, each was administered once daily for 1 week. Insulin resistance, blood glucose level, antioxidant markers and oxidative stress parameters were determined (Aldawsari et al., 2014).

2.13. Statistical analysis

Results were analyzed by using Excel data analysis applying *t*-test. Differences between formulations were considered to be significant at $p < 0.05$.

3. Results

3.1. Preliminary characterization parameters for both SLNs suspension and SLNs lyophilized powder

Table I shows the preliminary characterization parameters for both SLNs suspension ($F1_s$ – $F3_s$) and SLNs lyophilized powder ($F1_L$ – $F3_L$) extract formulations. Acceptable % sedimentation volume and % re-dispersibility values ranged from 83.833 – 91.833% and 95–100%, respectively for all formulations under test were obtained. An increase in viscosity was observed with increasing the amount of Compritol® for both SLNs suspension and reconstituted lyophilized SLNs formulations which was further explained by DSC studies. DSC diagrams of Compritol® and $F3_L$ are illustrated (Fig. 1). Slight melting point depression could be observed in the $F3_L$ formula (70.23 °C), compared to that of the Compritol® alone (72.57 °C).

Concerning the flowability and compressibility studies, the angle of repose, Hausner's ratio and Carr's index for $F3_L$ exhibited best values of 23.66°, 1.17 and 14.6% respectively.

3.2. Particle size analysis, zeta potential and surface morphology studies

In general, the nanoparticles were regular, and their shape ranged from completely spherical to subspherical with an acceptable particle size range (Fig. 2). The particle size of $F1_s$, $F2_s$, $F3_s$ SLNs suspension formulations (Table 2) was found to be 15.698, 26.966, 31.75 nm respectively. While for SLNs lyophilized formulations: $F1_L$, $F2_L$, $F3_L$ was 14.82, 22.73, 30.28 nm respectively (Table 2). It could be also observed that the particle size of both SLNs suspension and SLNs lyophilized formulations were significantly increased with increasing the amount of Compritol® in the formulation.

The zeta potential and poydispersity index (PDI) values are shown in Table 2. Results revealed that the $F3_s$ and its corresponding lyophilized formula $F3_L$ provided the lowest PDI values of 0.14 and 0.16, respectively. In addition, the same formulae showed the highest zeta potential values of −35.9 and −36.4, respectively.

3.3. % encapsulation efficiency (%EE), phenolic content and release behavior

All formulations under test exhibited an acceptable %EE and drug content ranged from 87.923 to 91.992 % and 95 to 100 %, respectively (Table 2). The release behavior of the phenolic content from suspension SLNs formulations is shown in Fig. 4 and for lyophilized SLNs formulations in Fig. 5 all compared to the extract. The release rate is getting slower with increasing the amount of Compritol® in both suspension and lyophilized SLNs formulations at $p < 0.05$. On the otherhand, all lyophilized formulations revealed burst liberation during the first points followed by a sustained release pattern (Fig. 6).

A) *P. acaciae* extract, $F1_s$ and $F1_L$
B) *P. acaciae* extract, $F2_s$ and $F2_L$
C) *P. acaciae* extract, $F3_s$ and $F3_L$

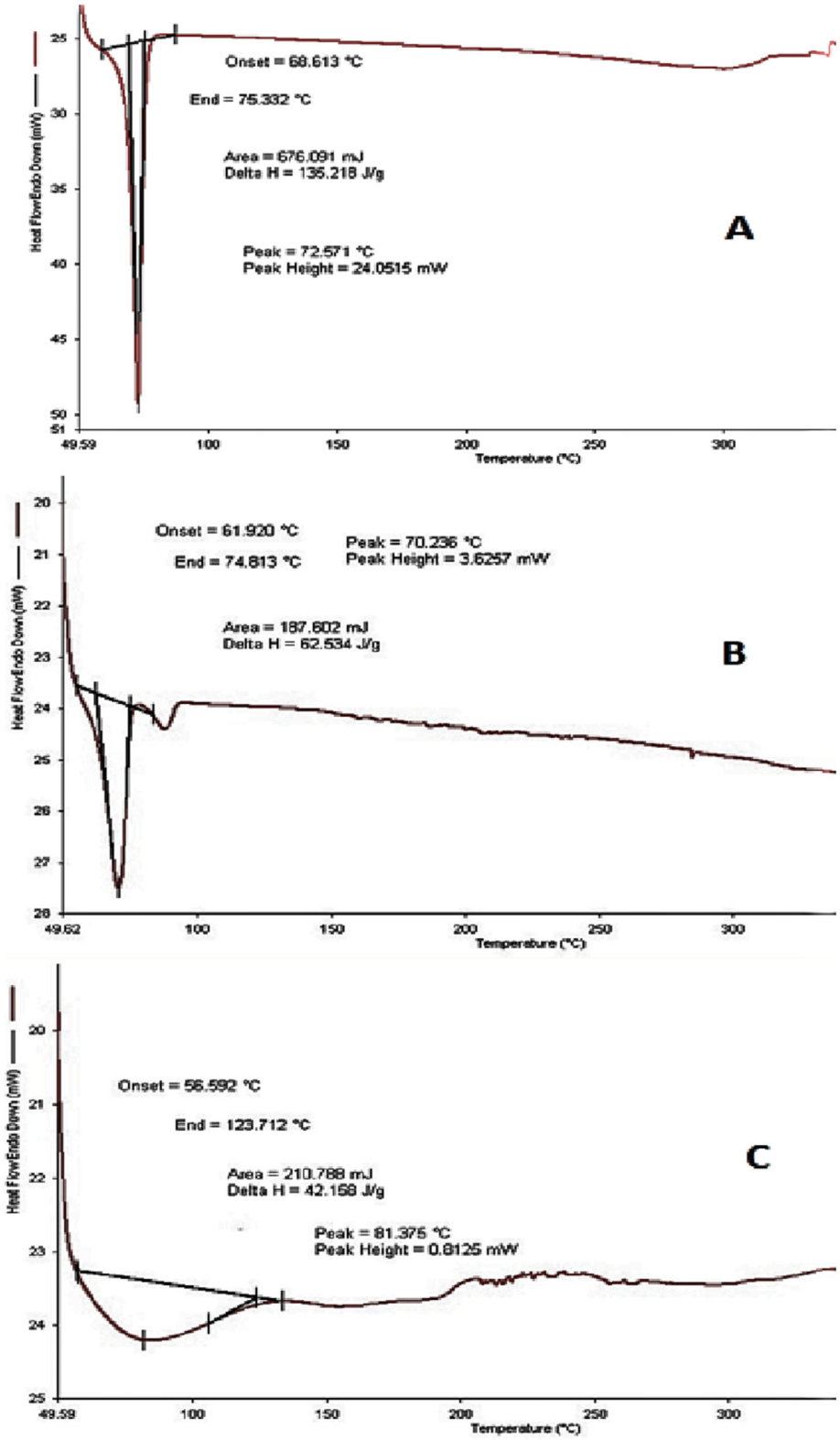

Fig. 1. DSC Diagram of A) DSC diagram of Compritol® B) DSC diagram of $F3_L$ C) *P. acaciae.*

3.4. Fourier transform infrared spectroscopic analysis (FTIR)

The FT-IR spectra of SLNs powder, pure Compritol®, pure extract, and physical mixture are demonstrated in Fig. 7. Compritol® FT-IR spectrum displays a characteristic broad stretching band at 3343.49 cm^{-1} for O–H bond. Other main band of C–H and ketonic stretching band of C = O bonds appear at 2919.10 and 1738.72 cm^{-1}, respectively (Shaveta et al., 2020) (Tatke et al., 2018). On the other hand, *P. acaciae* IR spectra revealed a characteristic band of stretching vibration broad O–H band of the major phenolic constituents of the extract among which; methyl gallate, catechin and quercetin at 3397.47 and 2933.7 cm^{-1}. Other O–H

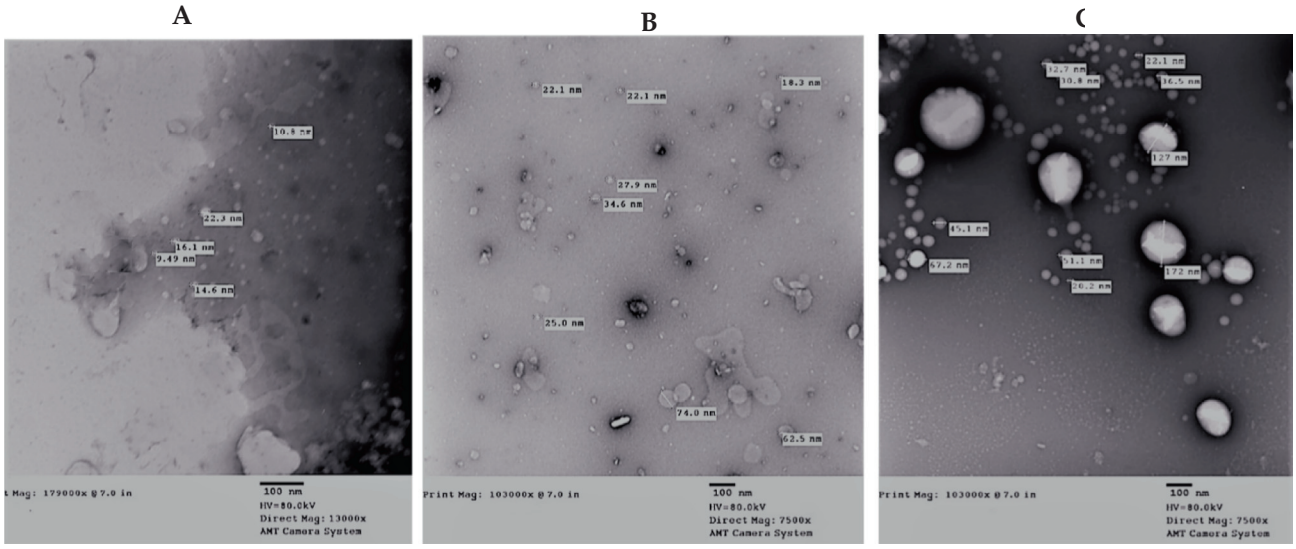

Fig. 2. TEM microphotographs for SLN suspension: A) $F1_s$ B) $F2_s$ C) $F3_s$.

Table 2
Characterization of both SLNs suspensions and lyophilized SLNs powder.

Code	Mean PS (nm) TEM	SD	Zeta potential (mV)	PDI	%EE	SD	Drug content (%)	SD
$F1_s$	15.698	5.187	−22.5	0.21	87.923	0.391	96.078	4.474
$F2_s$	26.966	3.842	−30.4	0.19	90.082	0.529	98.579	0.484
$F3_s$	31.75	5.050	−35.9	0.14	91.992	0.206	100.552	2.165
$F1_L$	14.82	4.02	−23.2	0.19	91.519	0.097	98.009	0.559
$F2_L$	22.73	4.84	−30.6	0.24	89.89	0.48	95.604	3.205
$F3_L$	30.28	5.17	−36.4	0.16	89.64	0.352	97.689	0.387

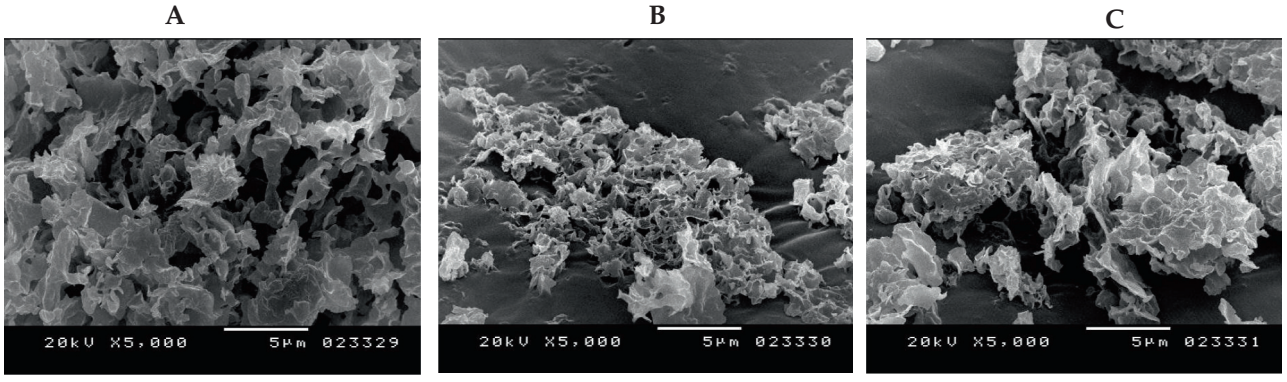

Fig. 3. SEM microphotographs for SLNs lyophilized formulations: A) $F1_L$ B) $F2_L$ C) $F3_L$.

bending bands appear at 1447.63 cm^{-1}, while the C = O ketonic aryl stretching band is observed at 1616.34 cm^{-1}.

4. Discussion

In our work, we aimed at preparing a free-flowing lyophilized powder of *P. acaciae* extract as a preliminary step for drug dosage form design either for reconstitution into suspension, filling into capsule, or compression into tablet. Preliminary characterization parameters for both SLNs suspension (F1s – F3s) and SLNs lyophilized powder ($F1_L$ – $F3_L$) extract formulations were examined. The increase in viscosity with increasing the amount of Compritol® in all formulations was observed.

Flowability parameters of lyophilized SLNs powdered formulations ($F1_L$ – $F3_L$) were tested to examine their suitability for formulation into tablet and/or capsule dosage form. The angle of repose, Hausner's ratio and Carr's index for $F3_L$ values were<30°, 1.25 and 15% respectively which indicate better flowability, compared to the other lyophilized SLNs powdered formulations (Hadi et al., 2016) (Singh et al., 2020) (Table 1).

TEM microphotographs of SLNs provide an idea about both the particles' shape and size. The non-significant difference in the particle size after lyophilization compared to their corresponding SLNs suspension formula, indicated the stability of the SLNs after lyophilization at $p < 0.05$. One of the factors affecting the PS of SLNs is the surfactant used in the preparation. The role of surfactant in nanoparticles preparation is to reduce the interfacial tension between the lipid and aqueous phase, and accordingly, the production of emulsion droplets of small size, leading to nanoparticles of small size. In addition, it affords stability to the SLNs by making a steric barrier on the particle surface, which protects nanoparticles from aggregation (H. Abbas et al., 2018). The acceptable PS range

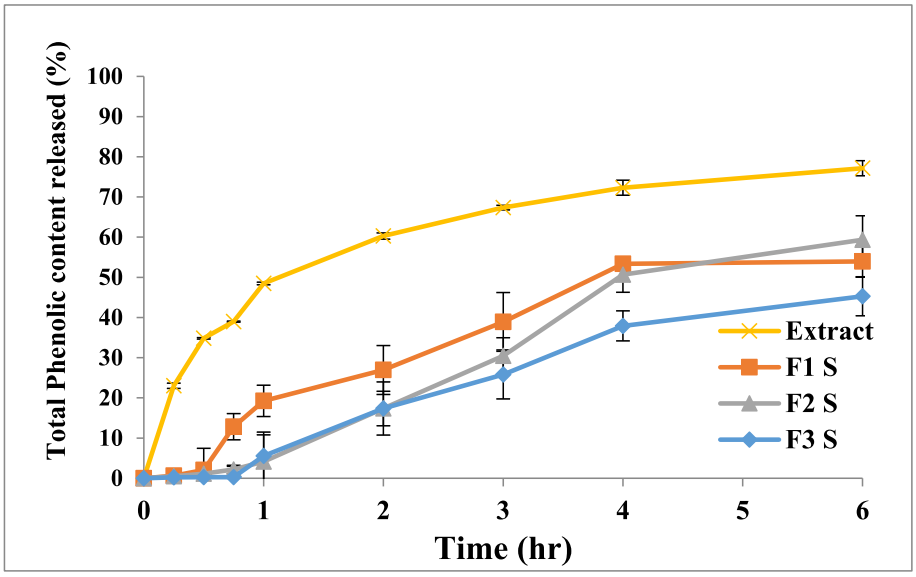

Fig. 4. The release behavior of *P. acaciae* extract, compared to SLNs suspension ($F1_S$, $F2_S$, $F3_S$) formulations.

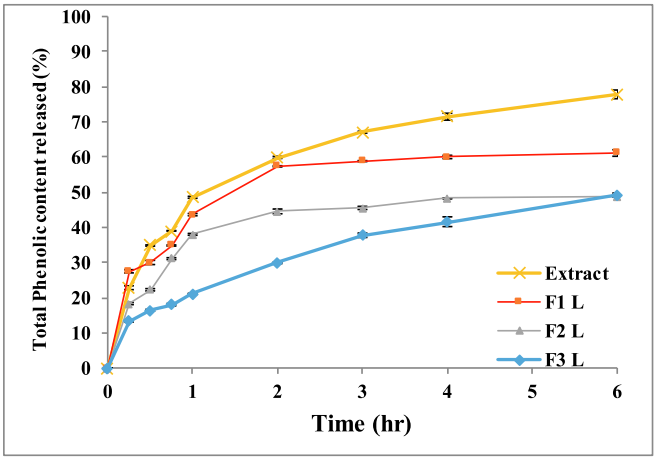

Fig. 5. The release behavior of *P. acaciae* extract, compared to lyophilized SLNs powder ($F1_L$, $F2_L$, $F3_L$) formulations.

obtained in all formulations indicates the powerful capability of the used surfactant (SDS) to lower the interfacial tension among Compritol® and aqueous phase during the emulsification step. It was previously reported that the PS obtained from Compritol® based γ-oryzanol SLNs using SDS as a surfactant, was about 170 nm using laser diffraction technique. However, using surfactant blend did not significantly reduce the diameter of SLNs (Karn-Orachai et al., 2016).

It was also observed that the size of both SLNs suspension and SLNs lyophilized formulations significantly increased with increasing the amount of Compritol® in the formulation. Compritol® existing as blend of mono-, di-, and triglycerides, together presented as triglyceride comprising long chain fatty acids responsible for its great hydrophobic character would explain the increase in P.S noticed with increasing its content in the formulation (Abou Youssef et al., 2018). This presumably is due to the increased interfacial tension between Compritol® and the aqueous external phase in the emulsion upon increasing the amount of Compritol® leading to increased particle size.

It's worth mentioning that the size dimensions achieved by TEM were much below than those achieved by light scattering procedure using Zetasizer. This finding was in agreement with many other researchers (El-Salamouni et al., 2018) (Hanafy et al., 2015) who related the reason to the way of sample preparation for TEM imaging which involves dehydration of the SLN. Whereas PS values obtained from Zetasizer determines the apparent size, which includes the aqueous layers surrounding the nanoparticles.

The polydispersity index is an important parameter in nanoparticles characterization as it reflects the degree of particles size uniformity. The value of PDI ranges between 0 and 1. The closer its value to zero, the greater is the similarity among the particles. Results revealed that the $F3_S$ and its corresponding lyophilized formula $F3_L$ provided the lowest PDI values of 0.14 and 0.16, respectively. In addition, the same formulae showed the highest zeta potential values of −35.9 and −36.4, respectively. Zeta potential is indicative to the SLN stability against agglomeration. As mentioned above, the surfactant on the SLNs surface can stabilize the system against aggregation by forming a steric barrier. In addition, being highly ionic, SDS layer covering the SLNs can generate an efficient electrostatic repulsion potential energy between the particles, and thus enhancing its stability against aggregation that would occur by the effect of intermolecular Van der Waals forces (H. Abbas et al., 2018). Comparable results were obtained in one study, where the zeta potential of the SLN formulation was significantly increased with increasing the concentration of sodium lauryl sulphate. Authors explained this result based on that anionic surfactants like SLS get adsorbed to the Helmholtz layer of SLN, thereby impart charge to the particle (Bhaskaran et al., 2022). A high zeta potential values; −51.5 and + 58.3 were reported for OZ-loaded SLNs using the ionic surfactants: SDS (anionic) and Cetylpyridinium chloride (cationic), respectively. Authors related this result to the strong residual charge for both ionic surfactants. On the other side, the nonionic surfactant; Tween 80, exhibited a significantly lower zeta potential of −19.3 (Karn-Orachai et al., 2016).

Concerning the % encapsulation efficiency and drug content, all formulations under test exhibited acceptable values (Table 2). As previously reported by our team (Aldawsari et al., 2014), the *P. acaciae* powder extract was prepared by maceration of the powdered dried plant material in methanol. Badr et al has also reported that the main component of the P acaciae extract, is its phenolic content including quercetin, catechin, rutin, gallic acid, methyl gallate, and loranthin (Badr et al., 2013). The first

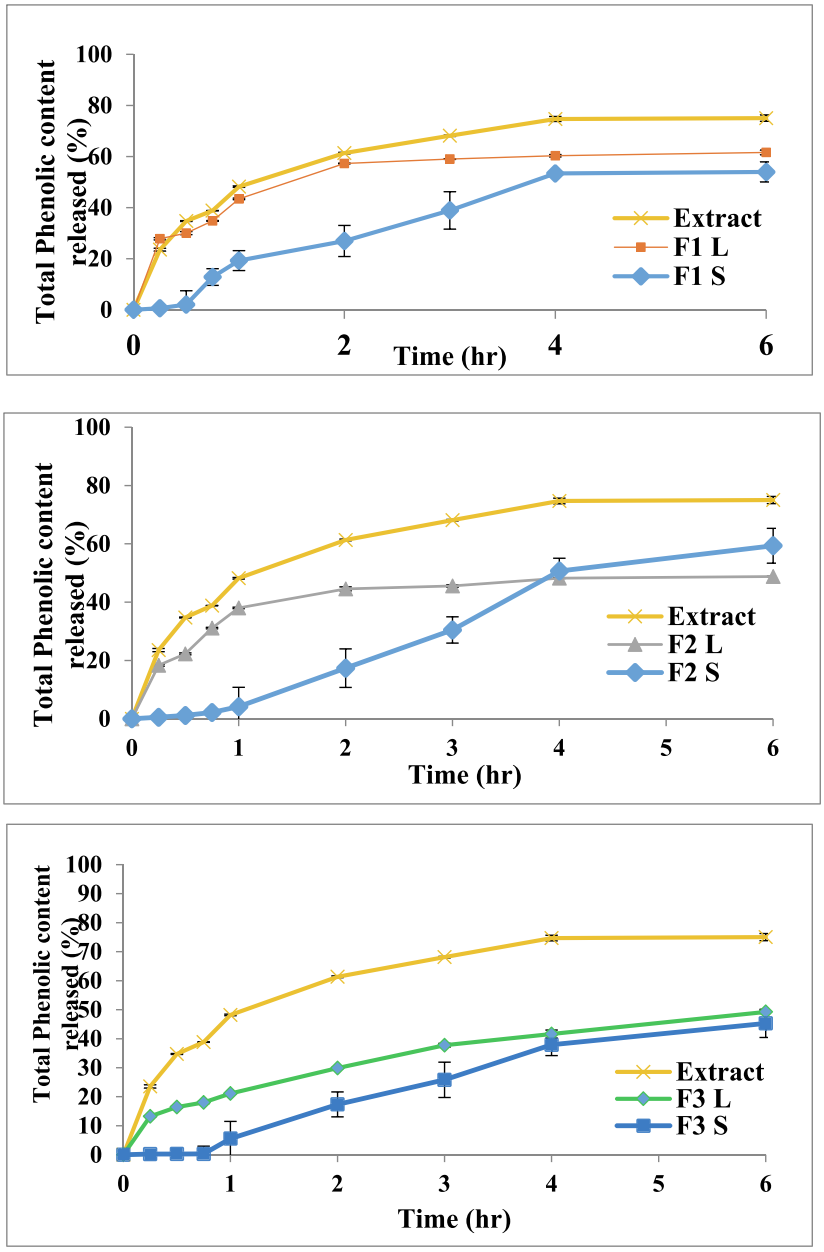

Fig. 6. The release behavior of *P. acaciae* extract, compared to both SLNs suspension ($F1_s$, $F2_s$, $F3_s$) and lyophilized SLNs powder ($F1_L$, $F2_L$, $F3_L$) formulations individually.

step for the powder extraction was maceration of the dried plant powder in methanol, followed by concentration under vacuum, and successive fractionation with hexane, chloroform, and ethyl acetate. In addition, quercetin was previously reported to possess poor aqueous solubility, as low as 0.55 μM. (Bose et al., 2013). From the previous, the poor aqueous solubility of the total phenolic content of the extract, could be concluded and the perfect entrapment of the phenolic components inside the prepared SLNs could be explained.

As previously mentioned, the release rate of the phenolic content from both suspension and lyophilized SLNs formulations compared to the extract became slower with increasing the amount of Compritol®. From the factors that contributes to the increased drug release from SLNs are the large effective surface area which is reflected by its small PS, reduced consistency in the matrix and a small diffusion distanced for the drug (zur Mühlen, Schwarz, & Mehnert, 1998). The drug release rate was reduced in SLNs with larger PS (Table 2) 15.698, 26.966, 31.75 nm for $F1_s$, $F2_s$, $F3_s$ and 14.82, 22.73, 30.28 nm for $F1_L$, $F2_L$ and $F3_L$, respectively. and higher viscosity (Table 1): 158.33, 306.33, 605.33 cp for $F1_s$, $F2_s$, $F3_s$ when compared to each other and 168, 311.33 and 764.33 cp also for reconstituted lyophilized ones.

In addition, it was previously reported that Compritol®, a solid lipid tends to produce firm particles, that limits the burst release of drug from a rigid matrix. Authors (Chaudhari et al., 2021) related the slow diffusion of quercetin (a phenolic ingredient and one of the *P. acaciae* extract components) from the nano-lipid carriers into the release medium to that reason, as it exhibited only 45% of its maximum release within 12 h.

The more porous surface of the $F1_L$ may also explain its higher release compared to both $F2_L$ and $F3_L$ (Fig. 3).

The biphasic release pattern; the initial step was burst release followed by a sustained one for all lyophilized formulations was comparable to those obtained by the authors (Rahman et al.,

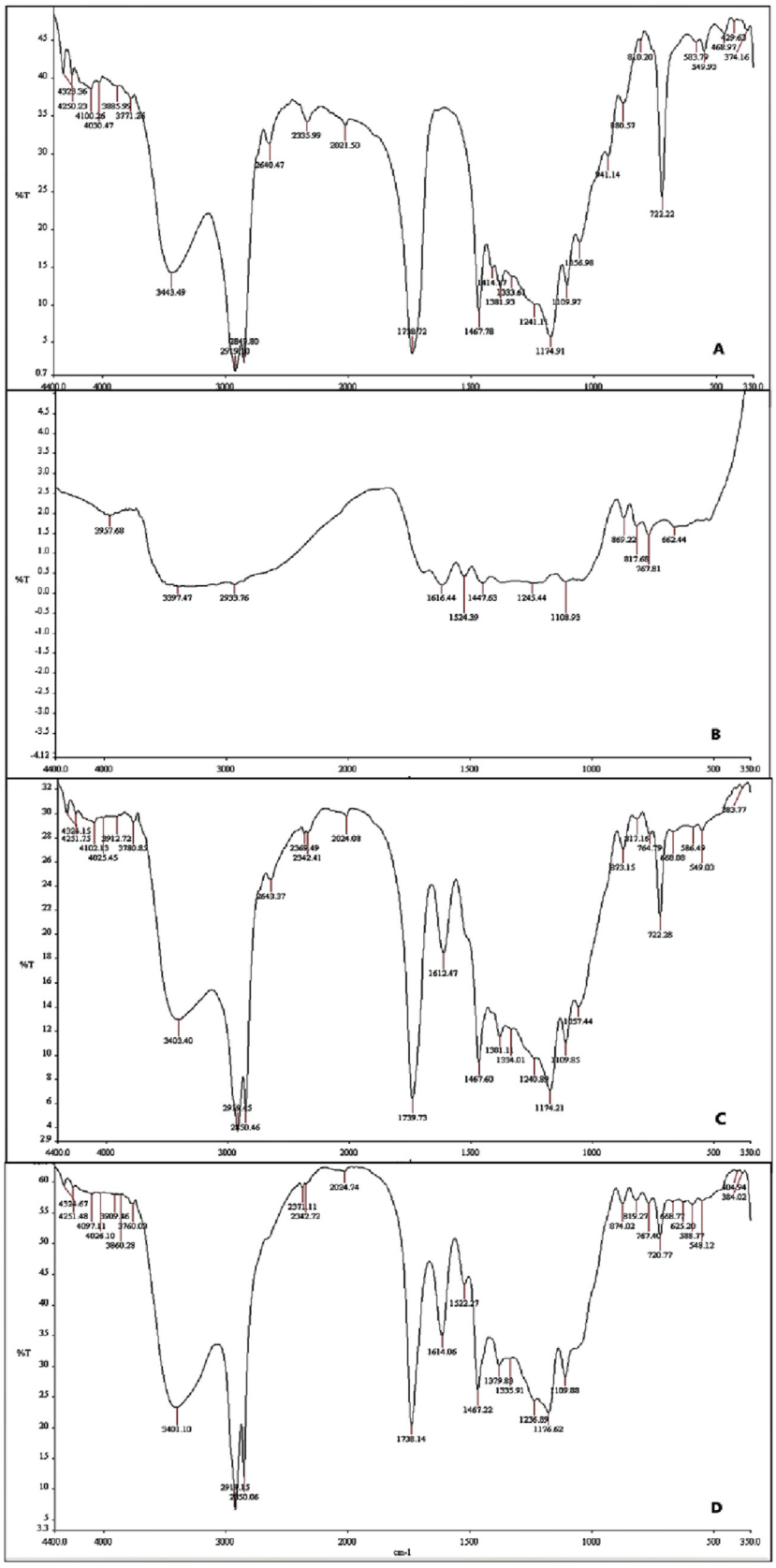

Fig. 7. IR spectra: A) Compritol, B) *P. acaciae* extract, C) Physical Mixture, D) SLN F3L.

2010) concerning the release of risperidone from Compritol 888 ATO based previously lyophilized and resuspended SLNs, using sodium lauryl sulphate as surfactant. Authors related this result to that the controlled release preparation usually demonstrates that biphasic release model and the burst liberation is perhaps due to the drug connected with the surface of the SLNs.

Learning drug release mechanisms and kinetics are essential in defining the drug diffusion profile or dissolution from a delivery system. In this context, the drug release data of the optimized preparation "$F3_L$" was aligned with the four models: first order, zero order, and Korsmeyer-Peppas and Higuchi equation. The release rate followed Higuchi diffusion model ($r^2 = 0.9912$) indicating the controlled release diffusion of the drug from the nanoparticle upon re-dispersion. Once the diffusion mechanism was ascertained by Higuchi model, Korsmeyer- Peppas indicated that the type of diffusion is Fickian affirmed by the diffusional release exponent n-value of 0.45 (Kunasekaran & Krishnamoorthy, 2015).

Fourier transform-infrared (FT-IR) spectrometry was utilized as an implement to find if there is any interaction between Compritol® and the extract. The physical mixture and formulation IR spectrum showed all peaks of both Compritol® and *P. acaciae* similar to those observed for the pure components indicating compatibility (Fig. 7). The slight variation in the peak intensities may be attributed to the overlapping of specific functional groups within a certain band width (O. M. Noman et al., 2019) (M. A. Noman et al., 2018). DSC studies showed slight melting point depression observed in the $F3_L$ formula, compared to that of the Compritol® alone. This result was in accordance with the previously reported finding where a more distinct melting point depression in Compritol® (71.1 °C) was noted after inclusion of prednisolone (67.6 °C) in comparison with etomidate (69.5 °C). This endorses the assumption of a molecular distributed state or an interstitial incorporation of the drug which lead to extra obvious drug–lipid interactions in the event of prednisolone inclusion (zur Mühlen et al., 1998).

5. Conclusion

The most stable suspension formulation $F3_s$ with highest Zeta potential value of −35.9 mV, exhibited also an acceptable PDI (0.14), PS (31.75 nm) and %EE (91.99%). So that it was lyophilized to obtain free flowing powder suitable for formulation ($F3_L$) into suspension for reconstitution, tablet, or capsule dosage forms. $F3_L$ was re-examined for the same parameters, to ensure its stability and it showed also acceptable results; ZP (-36.4 mV), PDI (0.16), PS (30.28 nm) and %EE (89.64 %).

As previously reported by our team, the whole extracts of *P. acaciae* and the SLNs preparations displayed a considerable blood glucose-reduction impact with antioxidant impacts in the diabetic rats type 2. The SLNs formulation with the greatest lipid content $F3_s$ provoked a significant lowering in glycated hemoglobin, the blood glucose level, and insulin resistance versus diabetic rats administered the oral hypoglycemic drug pioglitazone hydrochloride and with the group of rats that obtained *P. acaciae* extract. Authors related these findings to the high lipid content in $F3_s$ which may enhanced the procedure of permeation of the included extracts and also to the bioadhesion of SLNs to intestinal mucosa because of their tiny size, which could prolong their retention time. Decreasing hyperglycemia and insulin resistance in the diabetic rats was, at least partially, as a result of the antioxidant actions of the extracts and their SLNs preparations (Aldawsari et al., 2014). The obtained lyophilized SLNs is promising for preparation of a suitable stable dosage form for *P. acaciae* extract to be used in treatment of diabetes.

Author Contributions: All authors have read and agreed to the published version of the manuscript.

Funding

This research was funded by Princess Nourah bint Abdulrahman University Researchers Supporting Project number (PNURSP2023R165), Princess Nourah bint Abdulrahman University, Riyadh, Saudi Arabia.

Declaration of Competing Interest

The authors declare that they have no known competing financial interests or personal relationships that could have appeared to influence the work reported in this paper.

Acknowledgement

The authors extend their appreciation to Princess Nourah bint Abdulrahman University Researchers Supporting Project number (PNURSP2023R165), Princess Nourah bint Abdulrahman University, Riyadh, Saudi Arabia.

References

Abbas, H., Kamel, R., El-Sayed, N., 2018. Dermal anti-oxidant, anti-inflammatory and anti-aging effects of Compritol ATO-based Resveratrol colloidal carriers prepared using mixed surfactants. Int. J. Pharm. 541 (1–2), 37–47.

Abbas, M.A., Kandil, Y.I., Disi, A.M., Jaffal, S.M., 2019. Gastroprotective activity of Loranthus acaciae flower extract in a rodent model of ethanol-induced ulcer. Appl. Physiol. Nutr. Metab. 44 (12), 1283–1288.

Abou Youssef, N.A.H., Kassem, A.A., Farid, R.M., Ismail, F.A., Magda Abd Elsamea, E.-M., Boraie, N.A., 2018. A novel nasal almotriptan loaded solid lipid nanoparticles in mucoadhesive in situ gel formulation for brain targeting: preparation, characterization and in vivo evaluation. Int. J. Pharm. 548 (1), 609–624.

Aldawsari, H.M., Hanafy, A., Labib, G.S., Badr, J.M., 2014. Antihyperglycemic activities of extracts of the mistletoes Plicosepalus acaciae and P. curviflorus in comparison to their solid lipid nanoparticle suspension formulations. Zeitschrift für Naturforschung C 69 (9–10), 391–398.

Badr, J.M., Shaala, L.A., Youssef, D.T., 2013. Loranthin: A new polyhydroxylated flavanocoumarin from Plicosepalus acacia with significant free radical scavenging and antimicrobial activity. Phytochem. Lett. 6 (1), 113–117.

Bhaskaran, N.A., Jitta, S.R., Cheruku, S., Kumar, N., Kumar, L., 2022. Orally delivered solid lipid nanoparticles of irinotecan coupled with chitosan surface modification to treat colon cancer: preparation, in-vitro and in-vivo evaluations. Int. J. Biol. Macromol. 211, 301–315.

Bose, S., Du, Y., Takhistov, P., Michniak-Kohn, B., 2013. Formulation optimization and topical delivery of quercetin from solid lipid based nanosystems. Int. J. Pharm. 441 (1–2), 56–66.

Chakraborty, S., Shukla, D., Mishra, B., Singh, S., 2009. Lipid–an emerging platform for oral delivery of drugs with poor bioavailability. Eur. J. Pharm. Biopharm. 73 (1), 1–15.

Chaudhari, V.S., Murty, U.S., Banerjee, S., 2021. Nanostructured lipid carriers as a strategy for encapsulation of active plant constituents: Formulation and in vitro physicochemical characterizations. Chem. Phys. Lipids 235, 105037.

El Hajaji, H., Lachkar, N., Alaoui, K., Cherrah, Y., Farah, A., Ennabili, A., et al., 2010. Antioxidant properties and total phenolic content of three varieties of carob tree leaves from Morocco. Rec. Nat. Prod. 4 (4), 193.

El-Salamouni, N.S., Farid, R.M., El-Kamel, A.H., El-Gamal, S.S., 2018. Nanostructured lipid carriers for intraocular brimonidine localisation: development, in-vitro and in-vivo evaluation. J. Microencapsul. 35 (1), 102–113.

El-Sayed, M.-I.-K., Al-Massarani, S., El Gamal, A., El-Shaibany, A., Al-Mahbashi, H.M., 2020. Mechanism of antidiabetic effects of Plicosepalus Acaciae flower in streptozotocin-induced type 2 diabetic rats, as complementary and alternative therapy. BMC Complementary Medicine and Therapies 20 (1), 1–15.

Hadi, M.A., Rao, N.R., Rao, A.S., 2016. Formulation and evaluation of ileo-colonic targeted matrix-mini-tablets of Naproxen for chronotherapeutic treatment of rheumatoid arthritis. Saudi Pharmaceutical Journal 24 (1), 64–73.

Hanafy, A.S., Farid, R.M., ElGamal, S.S., 2015. Complexation as an approach to entrap cationic drugs into cationic nanoparticles administered intranasally for Alzheimer's disease management: preparation and detection in rat brain. Drug Dev. Ind. Pharm. 41 (12), 2055–2068.

Karn-Orachai, K., Smith, S.M., Saesoo, S., Treethong, A., Puttipipatkhachorn, S., Pratontep, S., Ruktanonchai, U.R., 2016. Surfactant effect on the physicochemical characteristics of γ-oryanol-containing solid lipid nanoparticles. Colloids Surf A Physicochem Eng Asp 488, 118–128.

Kelsey, N.A., Wilkins, H.M., Linseman, D.A., 2010. Nutraceutical antioxidants as novel neuroprotective agents. Molecules 15 (11), 7792–7814.

Kim, Y.-K., Kim, Y.S., Choi, S.U., Ryu, S.Y., 2004. Isolation of flavonol rhamnosides from Loranthus tanakae and cytotoxic effect of them on human tumor cell lines. Arch. Pharm. Res. 27 (1), 44–47.

Kumar, L., Reddy, M., Shirodkar, R., Pai, G., Krishna, V., Verma, R., 2013. Preparation and characterisation of fluconazole vaginal films for the treatment of vaginal candidiasis. Indian J. Pharm. Sci. 75 (5), 585.
Kunasekaran, V., Krishnamoorthy, K., 2015. Kinetic modeling of Rasagiline mesylate from nanoscale solid lipid particles. Int. J. Pharm. Pharm. Sci 7 (11), 300–305.
Labib, G.S., Aldawsari, H., 2015. Innovation of natural essential oil-loaded Orabase for local treatment of oral candidiasis. Drug Des. Devel. Ther. 9, 3349.
Lalitha, L.J., Sales, T.J., Clarance, P.P., Agastian, P., Kim, Y., Mahmoud, A., et al., 2020. In-vitro phytopharmacological and anticancer activity of Loranthus Longiflorus Desv. Var. Falcatuskurz against the human lung cancer cells. Journal of King Saud University-Science 32 (1), 1246–1253.
Leitão, F., Moreira, D.D.L., Almeida, M.D., Guimarães, L., 2013. Secondary metabolites from the mistletoes Struthanthus marginatus and Struthanthus concinnus (Loranthaceae). Biochem. Syst. Ecol. 48, 215–218.
Mehnert, W., Mäder, K., 2012. Solid lipid nanoparticles: production, characterization and applications. Adv. Drug Deliv. Rev. 64, 83–101.
Moglad, E.H., 2021. Loranthus acaciae: Alternative medicine for β-lactamase producer and methicillin-resistant Staphylococcus aureus. Saudi Journal of Biological Sciences 28 (3), 1835–1839.
Moglad, E.H., Hamad, A.M., Fatima, F., Seshadri, V.D., Naz, M., 2020. Antimicrobial and wound healing activities of certain Sudanese medicinal plants. Saudi Journal of Biological Sciences 27 (7), 1766–1772.
Mukherjee, S., Ray, S., Thakur, R., 2007. The current status of solid lipid nanoparticles. Pharmabit, XV 1, 53–60.
Mukherjee, S., Maity, S., Ghosh, B., Chakraborty, T., Mondal, A., Bishayee, A., 2020. Assessment of the antidiabetic potentiality of glyburide loaded glyceryl monostearate solid lipid nanoparticles. J. Drug Delivery Sci. Technol. 55, 101451.
Müller, R., Maaβen, S., Weyhers, H., Specht, F., Lucks, J., 1996. Cytotoxicity of magnetite-loaded polylactide, polylactide/glycolide particles and solid lipid nanoparticles. Int. J. Pharm. 138 (1), 85–94.
Müller, R.H., Mäder, K., Gohla, S., 2000. Solid lipid nanoparticles (SLN) for controlled drug delivery–a review of the state of the art. Eur. J. Pharm. Biopharm. 50 (1), 161–177.
Noman, O.M., Mothana, R.A., Al-Rehaily, A.J., Nasr, F.A., Khaled, J.M., Alajmi, M.F., Al-Said, M.S., 2019. Phytochemical analysis and anti-diabetic, anti-inflammatory and antioxidant activities of Loranthus acaciae Zucc. grown in Saudi Arabia. Saudi Pharmaceutical Journal 27 (5), 724–730.
Noman, M.A., Saif, A.A., Alburyhi, M.M., Al- Shibani, M.A., Al-Mahbshi, H.M., 2018. Pre-Formulation and Formulation Study of Plicosepalus acacia CapsulesDosage Forms. International journal of Pharmacy and Pharmaceutical Research 13 (4), 105–123.
Osadebe, P., Okide, G., Akabogu, I., 2004. Study on anti-diabetic activities of crude methanolic extracts of Loranthus micranthus (Linn.) sourced from five different host trees. J. Ethnopharmacol. 95 (2–3), 133–138.
Porter, C., Wasan, K.M., Constantinides, P., 2007. Lipid-based systems for the enhanced delivery of poorly water soluble drugs. Adv. Drug Deliv. Rev. 60 (6), 615–616.
Rahman, Z., Kohli, K., Khar, R.K., Ali, M., Charoo, N.A., Shamsher, A.A., 2006. Characterization of 5-fluorouracil microspheres for colonic delivery. AAPS PharmSciTech 7 (2), E113–E121.
Rahman, Z., Zidan, A.S., Khan, M.A., 2010. Non-destructive methods of characterization of risperidone solid lipid nanoparticles. Eur. J. Pharm. Biopharm. 76 (1), 127–137.
Rani, A.P., Hema, V., 2014. Formulation and Evaluation of Oxcarbazepine Suspension: In vitro/In vivo Correlation. Journal of Pharmaceutical Research International, 60–69.
Sadi, G., Güray, T., 2009. Gene expressions of Mn-SOD and GPx-1 in streptozotocin-induced diabetes: effect of antioxidants. Mol. Cell. Biochem. 327 (1), 127–134.
Sasidharan, S., Aravindran, S., Latha, L.Y., Vijenthi, R., Saravanan, D., Amutha, S., 2010. In vitro antioxidant activity and hepatoprotective effects of Lentinula edodes against paracetamol-induced hepatotoxicity. Molecules 15 (6), 4478–4489.
Shargorodsky, M., Debby, O., Matas, Z., Zimlichman, R., 2010. Effect of long-term treatment with antioxidants (vitamin C, vitamin E, coenzyme Q10 and selenium) on arterial compliance, humoral factors and inflammatory markers in patients with multiple cardiovascular risk factors. Nutr. Metab. 7 (1), 1–8.
Shaveta, S., Singh, J., Afzal, M., Kaur, R., Imam, S., Alruwaili, N., et al., 2020. Development of solid lipid nanoparticle as carrier of pioglitazone for amplification of oral efficacy: formulation design optimization, in-vitro characterization and in-vivo biological evaluation. J. Drug Delivery Sci. Technol. 57, 101674.
Shazhni, J.A., Renu, A., Vijayaraghavan, P., 2018. Insights of antidiabetic, anti-inflammatory and hepatoprotective properties of antimicrobial secondary metabolites of corm extract from Caladium x hortulanum. Saudi Journal of Biological Sciences 25 (8), 1755–1761.
Silva, A., González-Mira, E., García, M., Egea, M., Fonseca, J., Silva, R., et al., 2011. Preparation, characterization and biocompatibility studies on risperidone-loaded solid lipid nanoparticles (SLN): high pressure homogenization versus ultrasound. Colloids Surf. B Biointerfaces 86 (1), 158–165.
Silva, A., Kumar, A., Wild, W., Ferreira, D., Santos, D., Forbes, B., 2012. Long-term stability, biocompatibility and oral delivery potential of risperidone-loaded solid lipid nanoparticles. Int. J. Pharm. 436 (1–2), 798–805.
Singh, S.Y., Salwa, Shirodkar, R.K., Verma, R., Kumar, L., 2020. Enhancement in dissolution rate of atorvastatin trihydrate calcium by formulating its porous tablet using sublimation technique. J. Pharm. Innov. 15, 498–520.
Tatke, A., Dudhipala, N., Janga, K.Y., Balguri, S.P., Avula, B., Jablonski, M.M., Majumdar, S., 2018. In situ gel of triamcinolone acetonide-loaded solid lipid nanoparticles for improved topical ocular delivery: Tear kinetics and ocular disposition studies. Nanomaterials 9 (1), 33.
zur Mühlen, A., Schwarz, C., Mehnert, W., 1998. Solid lipid nanoparticles (SLN) for controlled drug delivery–drug release and release mechanism. Eur. J. Pharm. Biopharm. 45 (2), 149–155.